ISSN XXXX XXXX © 2016 IJESC

Research Article Volume 6 Issue No. 7

A New Three Level ZCS Soft Switching Boost DC-DC Converter for Solar PV System

Ahmed M. Kassem[1], Emad H. El-Zohri[2], Khairy Sayed[1], Alaa Abdelsamee[2]
Electrical Engineering Department, Faculty of Engineering, Sohag University, Sohag, Egypt[1]
Electrical Department, Faculty of Industrial Education Sohag University, Sohag, Egypt[2]

Abstract:
This paper proposes a new zero-current switching (ZCS) technique for three-level boost DC/DC converter. This new technique eliminates the switching loss and dv/dt noise due to the discharging of MOSFET's junction capacitances and the reverse recovery of diodes and enables the converters to operate at high frequencies. Consequently, the total turn-off switching losses can be significantly reduced and as a result, a high switching frequency of the used switches can be actually realized. The size and weight of the devices are reduced as the heat sink is not required. The effectiveness of the proposed converter topology is provided for PV system by the simulation results and power loss analysis using the simulation software PSIM.

Keywords: Three Level Boost Converter; Resonant switches; Zero-current switching.

1. INTRODUCTION

During the last period, with the scientific development of power electronics devices, development of control techniques, small size and the increasing demand of high-quality power supply, power electronics technology has invoked the widely attention from research scholars over the world. Power electronics technology has been gradually taken up in civilian industrial areas to cope with these demands. The various converters for different requirements are developed and related technology is studied by scientists to accomplish the research of new converters [1-3]. A power electronic converter contains elements such as energy storage inductors, capacitors and transformers, which represents a large part of the total volume. These components are used to store and transfer energy as a part of the energy conversion process. As the switching frequency of the converter increases, the constituent elements of energy storage values go down, as do the physical size and weight, due to the shorter time they are required to store the voltage or the current. As a result, the high frequency shift adapter works with the smallest elements of the energy storage (and thus the overall size).

In the case of overlap between the switching voltage wave and wave current, this leads to increased conversion losses and increased generation EMI (Electromagnetic Interference). The loss appears in every switching cycle. Therefore, its loss increases as the switching frequency increases and the operational voltage increases. It is therefore essential to reduce the switching losses by employing resonant switching techniques. Therefore, focusing on the overall system performance, its size, weight, efficiency and power conversion density, Resonant Transition Converter topology were found to be suitable to operate at high frequencies [4-8].

By using the three level boost topology in the high power and high voltage applications, significant advantages will be achieved over the conventional boost converter. With the three level boost converter, the inductance of the boost inductor can be greatly reduced, and the semiconductor device voltage rating is only half of the output voltage. As a result, the converter power density and efficiency will be significantly improved, and the cost will be reduced for high power and high voltage applications [8-10].

Photovoltaic system is an optical system to convert sunlight directly into electricity. The main body of the optical system is the photovoltaic cell. The cells can be grouped to form panels or modules. The plates can be grouped to form large photovoltaic arrays. Usually it employs the term to describe the collection plate photovoltaic (with several cells connected in series and / or parallel) or a set of plates converts sunlight into electricity. The main body of the optical system is the photovoltaic cell. The cells can be grouped to form panels or modules. The plates can be grouped to form large photovoltaic arrays. Usually it employs the term to describe the collection plate photovoltaic (with several cells connected in series and / or parallel) or a set of plates [11]. The term array used henceforth means any photovoltaic device composed of several basic cells. The use of new, efficient photovoltaic solar cells (PVSCs) has emerged as an alternative measure of renewable green power, energy conservation and demand-side management [12, 13].The main technical requirements in the development of a practical PV system are: (A) optimal control that can be the maximum power output of PV arrays under all operating conditions and the weather, and (B) a high rate of performance for those who extract cost to facilitate the marketing of advanced PV technologies. Since PV arrays have a very non-linear property, and changes its performance with operating conditions such as the sun or room temperature, it is technically difficult to develop the PV system that can meet the technical requirements [14].

2. PROPOSED SOFT-SWITCHING THREE-LEVEL (DC-DC) CONVERTER

For three-level Boost converter, only the case when the inductor current is continuous is discussed here. Fig.1 shows the main circuit of the three-level Boost converter, wherein Q_1 and $Q_2$are switch tubes, D_1, D_2 are the Boost diodes, L_1, L_2 are the Boost inductors, C_1, C_2 are the two output voltage dividing capacitors, its power capacity is larger and equal to half of the

output voltage, R_L is loaded. Q_1, Q_2 alternately works, the difference between the drive signal is 180.

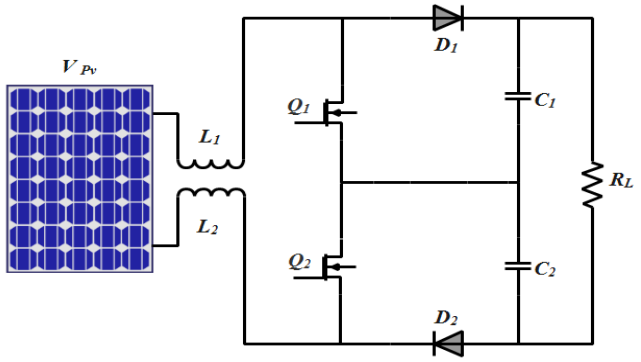

Fig.1: Conventional Three-level Boost Converter

The power converter can be operated with high conversion frequencies unless they shift losses problems can be overcome. This can be done using "soft switch" techniques. The term "soft switch" refers to various techniques that make transformations to convert more gradual than just simply turning switches on or off (which is referred to as "hard to shift" in literature, electronics and electricity) and this force either voltage or current to be zero while the switching transition is being made [9, 10]. Switching losses are reduced as there is no overlap switch voltage and current transformation during a transition period switch her one of the two zero during this time. Soft switching techniques either zero-voltage-switching (ZVS) techniques or switching (ZVS) zero current techniques [10].

The proposed converter aims to provide the ZVS to the main switches. This is done by adding auxiliary devices to the classical converter. The auxiliary device is also needed to switch under ZVS by itself, so that no additional switching loss will be occurred in the creation of the ZVS circuit [5]. Figure 2 shows two configurations of switches. Fig. 2a is a current mode resonant switch and Fig. 2b is a voltage mode switch. A current mode switch is for zero current switching (ZCS) and a voltage mode switch is for zero voltage switching (ZVS).

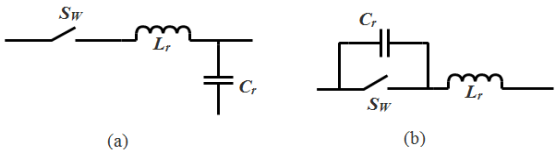

Fig. 2: Resonant switches (a) zero-current switching (b) zero-voltage switching

It can be seen that a capacitor ***Cr*** is connected in parallel with SW for ZVS whereas Lr is connected in series with ***SW*** for ZCS. This resonant capacitor ***Cr*** will resonate to zero voltage before ***SW*** turns on. On the other hand, when the switch is turned off, considerable time is required to charge ***Cr*** from zero voltage and hence the voltage across the ***SW*** is not increased instantaneously. The overlapping between the current and voltage of ***SW*** is therefore very small. This is why zero voltage turn-off can be achieved. The general characteristic of ZVS is that there is a resonant capacitor connected directly in parallel with the switch whereas the general characteristic of ZCS is that there is a resonant inductor connected directly in series with the switch [6].

There are two ways to implement this resonant switch. Fig. 2a is a general configuration. Fig. 2b is a half-wave mode where the resonant voltage is only uni-directional because the anti-parallel diode behaves as short-circuit when the voltage across ***Cr*** makes it forward-bias. It therefore stops its voltage from reversing. Fig. 3c is full-wave mode where the resonant voltage is bidirectional because the series diode ***D*** disables any body diode of the transistor, for example power MOSFET. Any resonant voltages across ***Cr*** can resonate in both directions [5].

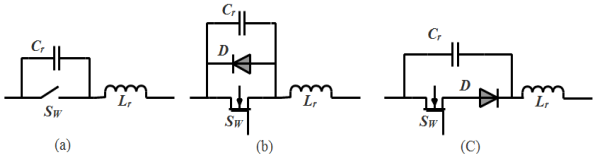

Fig. 3: Configurations of the zero-voltage switch (a) general (b) half-wave (c) full-wave

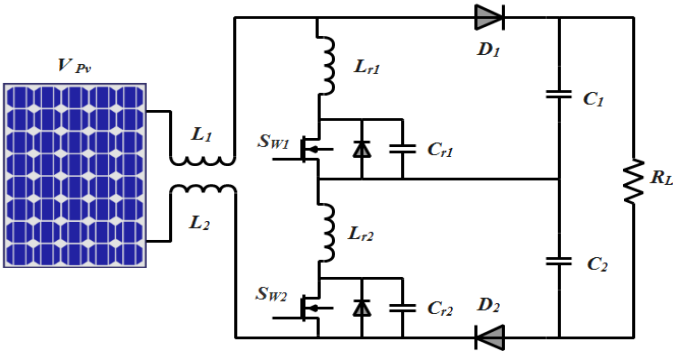

Fig. 4: Proposed soft switching three-level boost converter

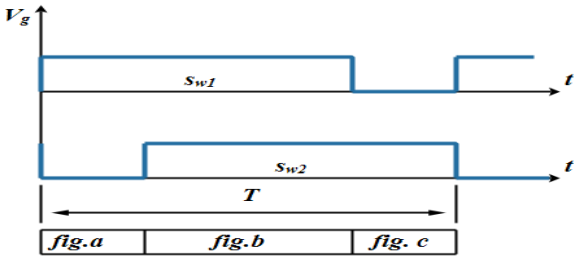

Fig. 5: Gate pulse sequences

The resonant power converter utilizes the resonance theory by incorporating an ***LC*** resonant circuit as shown in Fig. 4 from the conventionally adopted PWM converter with the gate pulse sequences shown in Fig. 5. The switching-on and switching-off instants of power switch occurs at zero voltage, it will help to reduce the switching losses, switching stress, ***dv/dt*** and ***di/dt*** surge, and thus EMI.

The circuit consists auxiliary Diode ***D*** is connected across the switch with the appropriate polarity to ensure turned on instant of power switch at zero voltage. The Inductor L_r is connected in series with power switch ***SW*** to limit ***di/dt*** of the power switch and the capacitor C_r is connected across the switch to limit ***dv/dt*** of the power switch. Inside ZVS Three level boost converter, soft-switching is applied to the power switch. Because of this special feature ZVS buck converter is suitable for high-frequency conversion applications [7].

3. OPERATION PRINCIPLE

The ZVS is used during a turn ON of the device. Initially the main switch is OFF and the auxiliary switch is ON. So the current through the main switch is zero, but the voltage is not zero. During the turn ON, voltage is made zero and current is given some time delay so that the current will begin to rise

after the voltage is zero [8]. Fig. 6 presents switch waveforms on the proposed soft switching three level boost converter.

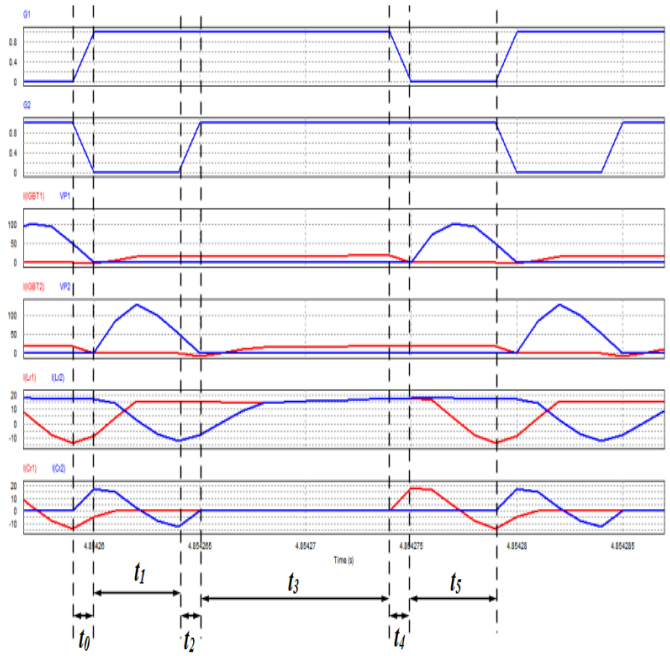

Fig. 6 Waveforms of the three level boost converter

Mode 1: at (t_0) - in this mode S_{W1} Is turn ON and S_{W2} Is turn OFF as shown in figure (7 - 1), A decrease the value of voltage flowing in the S_{W2} To zero voltage and drop-in the value of current flowing in the S_{W2} to zero current value.

Mode 2: at (t_1) - in this mode S_{W1} Is ON and S_{W2} Is OFF as shown in figure (7 - 2). In the S_{W1} Current starts to increase until it reaches the maximum value so organized and so with the stability of the voltage value zero, in the S_{W2} Starts the voltage from zero increases up any maximum values him, then decline to near zero volts, and so with the stability of the current value of zero.

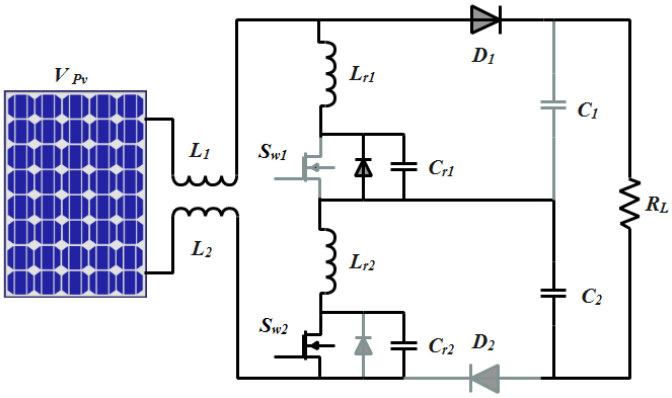

Mode (1)

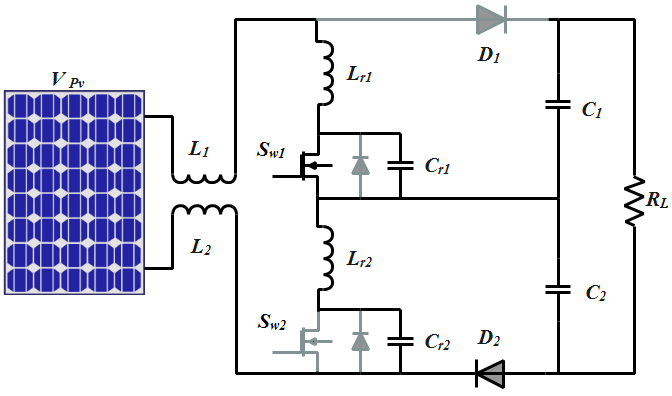

Mode (2)

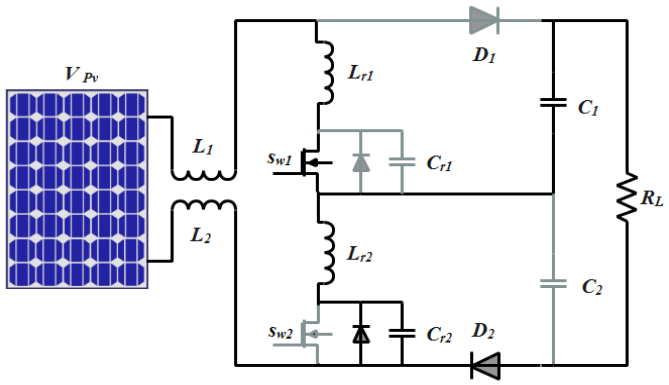

Mode (3)

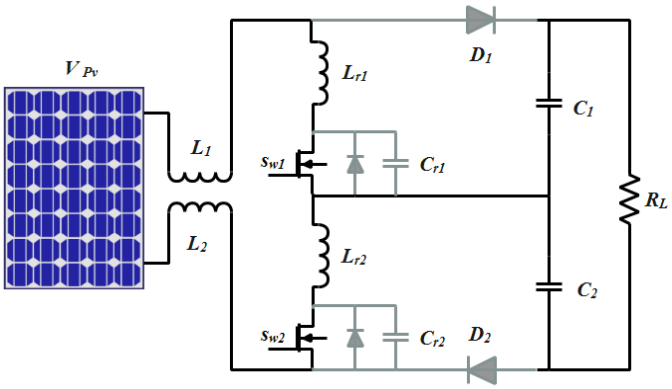

Mode (4)

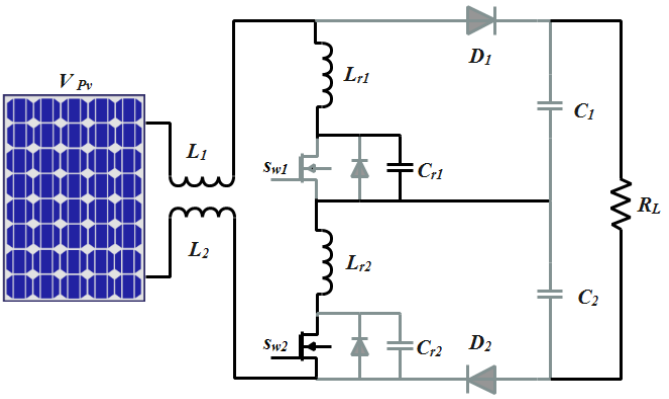

Mode (5)

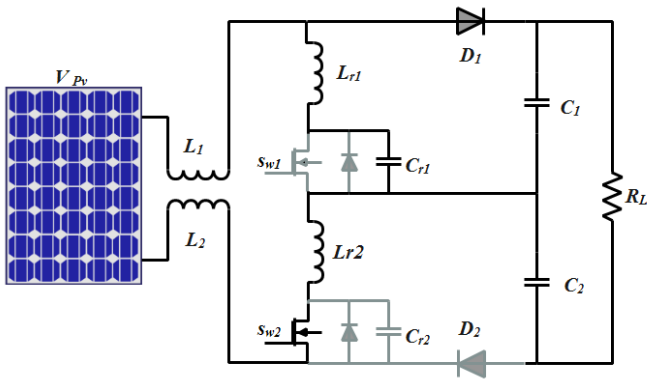

Mode (6)

Fig. 7 : Equivalent circuits of the proposed soft switching three level boost converter in each operation mode

Mode 3: at (t_2) - in this mode S_{W1}Is ON and S_{W2} Is turn ON as shown in figure (7 - 3). In the S_{W1}With the stability of the current value when the maximum value, in the S_{W2} Decrease in the value of the voltage until it reaches zero volts.

Mode 4: at (t_3) - in this mode S_{W1}Is ON and S_{W2} Is ON as shown in figure (7 - 4). In the S_{W1}With the stability of the current value when the maximum value, in the S_{W2} Current starts to increase until it reaches the maximum value so organized and so with the stability of the voltage value zero.

Mode 5: at (t_4) - in this mode S_{W1} Are turn OFF and S_{W2} Is ON as shown in figure (7 - 5). In the S_{W1} Decrease in the current value until it reaches zero current, in the S_{W2} With the stability of the current value when the maximum value.

Mode 6: at (t_5) - in this mode S_{W1} Is OFF and S_{W2} Is ON as shown in Fig. (7 - 6). In the S_{W1} Starts the voltage from zero increases up any maximum values him, then decline to near zero volts, and so with the stability of the current value at zero, in the SW2 With the stability of the current value when the maximum value.

$$\left.\begin{aligned} v_l &= v_{L1} + v_{L2} \\ v_l &= V_{pv} - v_{c2} - v_{L_{r1}} \\ i_{c1} &= -\frac{V_O}{R} \\ i_{c2} &= I_l - \frac{V_O}{R} \end{aligned}\right\} \qquad (1)$$

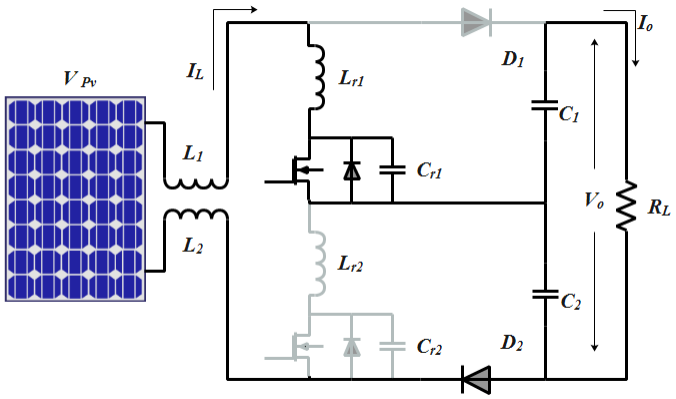

Fig. 8(a)

$$\left.\begin{aligned} v_l &= V_{pv} - v_{L_{r1}} - v_{L_{r2}} \\ i_{c1} &= i_{c2} = -\frac{V_O}{R} \end{aligned}\right\} \qquad (2)$$

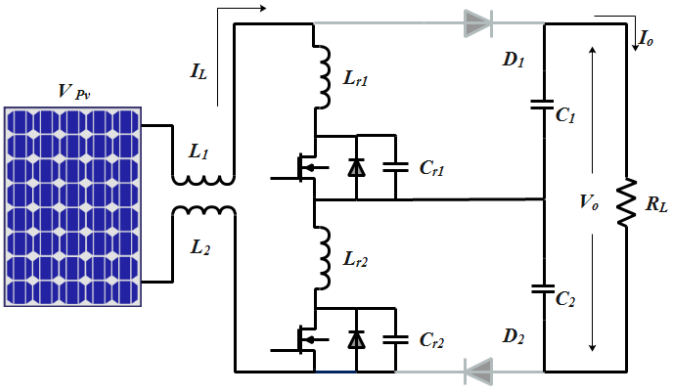

Fig. 8(b)

$$\left.\begin{aligned} v_l &= V_{pv} - v_{L_{r2}} - v_{c1} \\ i_{c1} &= I_l - \frac{V_O}{R} \\ i_{c2} &= -\frac{V_O}{R} \end{aligned}\right\} \qquad (3)$$

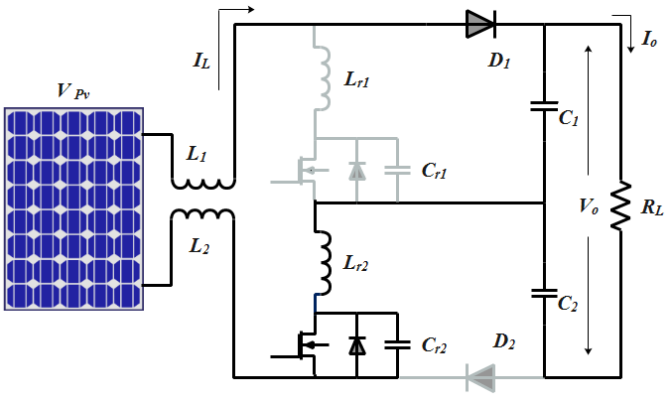

Fig. 8(c)

Fig. 8: Loss model for each operation state of the two-level boost converter: a. Inductor is charging, b. Capacitor 1 charging and c. Capacitor 2 charging

Following the above switching modality we proceed to derive the voltage relationship, the inductor and capacitor size equations.

$$v_{c1} = v_{c2} = \frac{1}{2}V_O \qquad (4)$$

From the inductor volt-second balance equation, we obtain the relationship of the voltages as a function of the duty cycle **D**:

$$\frac{V_0}{V_{pv}} = \frac{2}{(1-D)} \qquad (5)$$

And from the capacitor charge balance equation

$$I_l = \frac{2V_0}{(1-D)R} \qquad (6)$$

We can also then derive the inductance formula for a constant load and duty cycle. This leads to

$$L = \frac{R(1-D)D}{8f} \qquad (7)$$

And then the capacitance formula for a constant load is as follows,

$$C = \frac{V_0 D}{4Rf\Delta v} \qquad (8)$$

For a variable input voltage, output voltage and load that follows the relationships

$$V_{Pv_{min}} < V_{Pv} < V_{pv_{max}}$$

$$V_{0_{min}} < V < V_{0_{max}}$$

$$P_{min} < P < P_{max}$$

The duty cycle is,

$$D = 1 - 2\frac{V_{pv}}{V_0} \qquad (9)$$

From (9) we can see that to have a positive and non-zero duty cycle $V_o > 2V_{Pv}$ therefore, $V_{o_{min}} > 2V_{pv_{max}}$. Then the inductance is,

$$L = \frac{V_O D(1-D)^2}{16 f I_{load}} \qquad (10)$$

And the capacitance is the same as in equation (8).
With these additions, equations (1, 2 and 3) are modified as follows

• Inductor is charging (States 1 and 3, Figure 1a)

$$\left.\begin{aligned} v_l &= V_{pv} - I_l R_l - V_{s1} - V_{L_{r1,2}} - V_{s2} \\ i_{c1} &= i_{c2} = -\frac{V_O}{R} \end{aligned}\right\} \qquad (11)$$

• Capacitor 1 charging (State 2, Figure 1b)

$$\left.\begin{aligned} v_l &= V_{pv} - I_l R_l - v_{c1} - V_{s2} - V_{L_{r2}} - V_D \\ i_{c1} &= I_l - \frac{V_O}{R} \\ i_{c2} &= -\frac{V_O}{R} \end{aligned}\right\} \qquad (12)$$

• Capacitor 2 charging (State 4, Figure 1c)

$$\left.\begin{aligned} v_l &= V_{pv} - I_l R_l - V_{s1} - V_{L_{r1}} - v_{c2} - V_D \\ i_{c1} &= -\frac{V_O}{R} \\ i_{c2} &= I_l - \frac{V_O}{R} \end{aligned}\right\} \qquad (13)$$

Then, following the switching pattern presented in Fig. 2, for $v_{c1} = v_{c2} = \frac{1}{2}V$, $V_s = V_{s1} = V_{s2}$ and $V_{L_r} = V_{L_{r1}} = V_{L_{r2}}$, the inductor volt-second balance equation yields

$$V_{pv} - I_l R_l - (1+D)(V_s + V_{L_r}) - {}^1\!/_2 \acute{D} V_O - \acute{D} V_D = 0 \qquad (14)$$

From equation (14) and replacing I_l as in equation (6), we obtain

$$\frac{V_O}{V_{pv}} = \frac{2}{\acute{D}}\left[1 - (1+D)\frac{(V_s+V_{L_r})}{V_{pv}} - \acute{D}\frac{V_D}{V_{pv}}\right]\left[\frac{1}{1+\frac{4R_L}{(\acute{D})^2 R}}\right] \qquad (15)$$

The efficiency of the converter is obtained calculating

$$\eta = \frac{P_{out}}{P_{in}}$$ where,

$$P_{in} = V_{pv} . I_l \qquad (16)$$

$$P_{out} = V_O . I_O = V_O\left({}^1\!/_2 \acute{D} I_l\right) \qquad (17)$$

Therefore,

$$\eta = \frac{V_O\left({}^1\!/_2 \acute{D} I_l\right)}{V_{pv} . I_l} \qquad (18)$$

$$\eta = \left[1 - (1+D)\frac{(V_s+V_{L_r})}{V_{pv}} - \acute{D}\frac{V_s}{V_{pv}}\right]\left[\frac{1}{\frac{4R_l}{(\acute{D})^2 R}}\right] \qquad (19)$$

4. MODELING AND SIMULATION

A Photovoltaic (PV) system directly converts solar energy into electrical energy. The basic device of a PV system is the PV cell. Cells may be grouped to form arrays. The voltage and current available at the terminals of a PV device may directly feed small loads such as lighting systems and DC motors or connect to a grid by using proper energy conversion devices. This photovoltaic system consists of main parts such as PV module, charger, battery, inverter and load [15]. A Photovoltaic cell is a device used to convert solar radiation directly into electricity. It consists of two or more thin layers of semiconductor material, most commonly silicon. When the silicon is exposed to light, electrical charges are generated. A PV cell is usually represented by an electrical equivalent one-diode model shown in Fig. 9 [16].

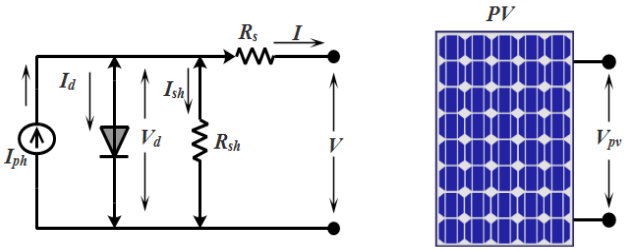

Fig. 9: Equivalent circuit of PV solar cell

The output current I of solar arrays am given by (1) using the symbols in Fig. 9.

$$I = I_{ph} - I_d - \frac{V_d}{R_{sh}} \qquad (1)$$

$$V_d = V + R_s I \qquad (2)$$

$$I_d = I_o\left\{e^{\left(\frac{q V_d}{nKT}\right)} - 1\right\} \qquad (3)$$

Where,

I_{ph} Is the photocurrent (in amperes)

I_d Is the diode current (in amperes)

I_o Is the reverse saturation current (in amperes)

R_s Is the series resistance (in ohms)

R_{sh} Is the parallel resistance (in ohms)

n Is the diode factor

q Is the electron charge $q = 1.6 * 10^{-19}$ (in coulombs)

k Is Boltzmann's constant (in Joules/ Kelvin)

T Is the panel temperature (in Kelvin).

V Is the cell output voltage (Volts)

V_d Is the diode voltage (Volts)

The output current I after eliminating the diode components is expressed as

$$I = I_{ph} - I_o\left\{e^{\left(\frac{q V_d}{nKT}\right)} - 1\right\} - \frac{V + I R_s}{R_{sh}} \qquad (4)$$

4.1. Maximum Power Point Tracking (MPPT) Techniques:

The tracking algorithm works based on the fact that the derivative of the output power P with respect to the panel voltage V is equal to zero at the maximum power point. The module P-V characteristics are shown in Fig. 10 show further that the derivative is greater than zero to the left of the peak point and is less than zero to the right.

$$\frac{\partial P}{\partial V} = 0 \quad for \quad V = V_{mp} \qquad (i)$$

$$\frac{\partial P}{\partial V} > 0 \quad for \quad V < V_{mp} \qquad (ii)$$

$$\frac{\partial P}{\partial V} < 0 \quad for \quad V > V_{mp} \qquad (iii)$$

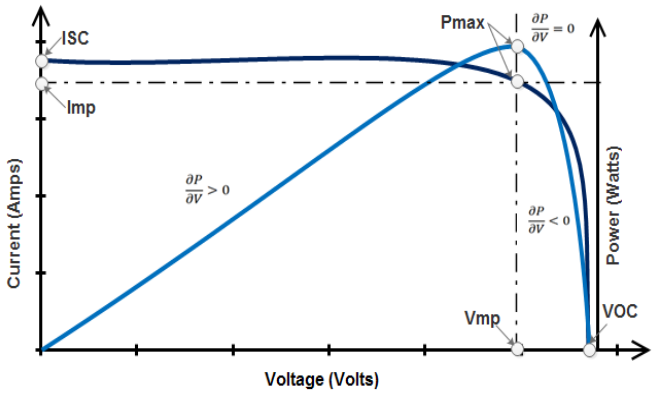

Fig. 10: P-V Characteristics of a module [17].

In the literature, various MPPT algorithms are available in order to improve the performance of PV systems by effectively tracking the MPPT. However, most widely used MPPT algorithms are considered here.

4.2. PERTURB AND OBSERVE (P&O):

The most commonly used MPPT algorithm is P&O method and is also known as hill climbing algorithm. This technique employs simple feedback arrangement and few measured parameters. In this approach, the array voltage is periodically given a perturbation and the corresponding output power is compared with that at the previous perturbation cycle. However, the operating point oscillates around the MPP as the system is continuously perturbed. This method can be implemented easily as shown in Fig. 11 [17].

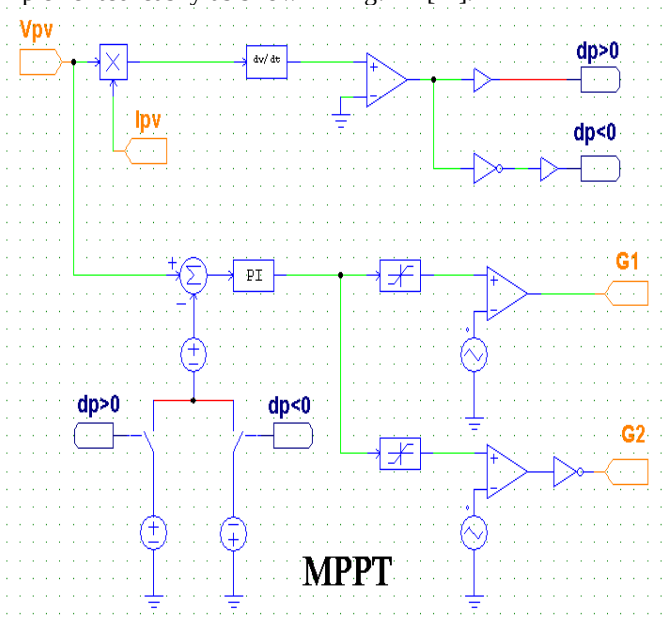

Fig. 11: Implementation of P&O technique

In this simple algorithm, the operating voltage is perturbed with a small change +ΔV and the power output is observed. Depending on the sign of observed power, further perturbation will be given to voltage as described in Fig. 12.

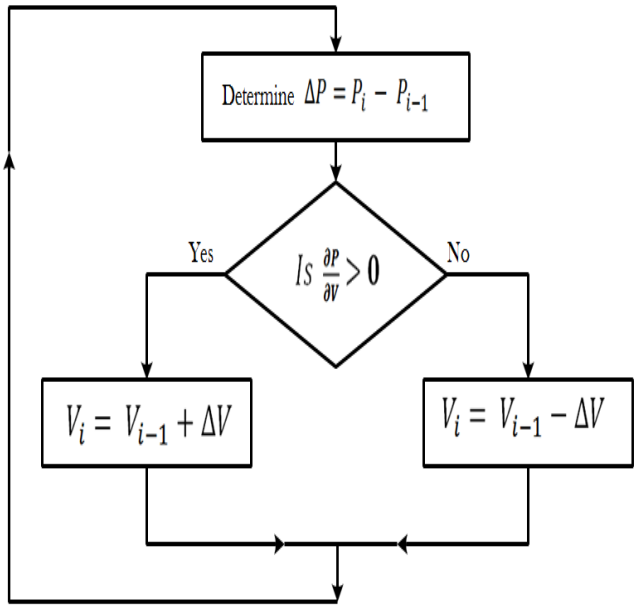

Fig. 12: P&O flow chart [17].

5. Simulation results

Simulations have been carried out on the circuit shown in Fig. 13 using the simulation software PSIM. The P & O technology is used on a large scale because of the P & O simplicity of implementation as it is shown in Fig. 12. Major circuit parameters are listed in Table I. Figure 14 shows the waveforms of the voltage V_{pv}, current I_{pv} and the power output P_{pv} of PV cells. Figure 15 shows the waveforms of the output voltage V_{out} and output current I_{out} and output power P_{out} for process simulation of the proposed circuit. The simulation shows that the output voltage 286.57 volts and the output current of 0.75 amperes and the power output 216.11 Watt as well as achieving an efficiency of 91.5%. This clearly shows that the proposed technique is effective and efficient.

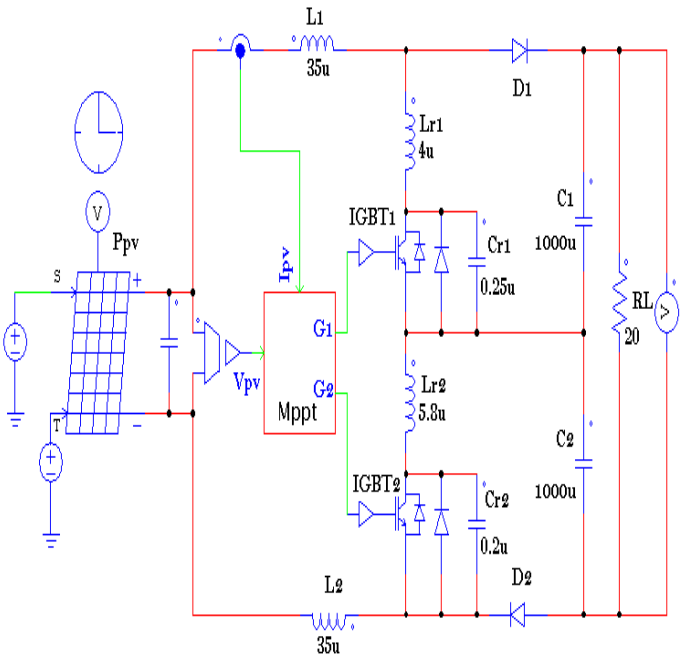

Fig. 13: Simulation diagram of the system

Table I: Circuit Parameters

Item	Symbol	Value
Input Voltage	V_{in}	44 V
Output Voltage	V_{out}	286.5 V
Switching Frequency	f_{sw}	4 KHz
Load Resistance	R_L	380 Ω
Filter Capacitor	C_1 , C_2	1000µf
Input inductor	L1 ,L2	35µH
Resonant capacitor	Cr1 ,Cr2	0.25µf , 0.2µf
Resonant inductor	Lr1,Lr2	4µH , 5.8µH
MOSFET	Q1 , Q2	IRFP250
DIODES	D1 , D2	10A01

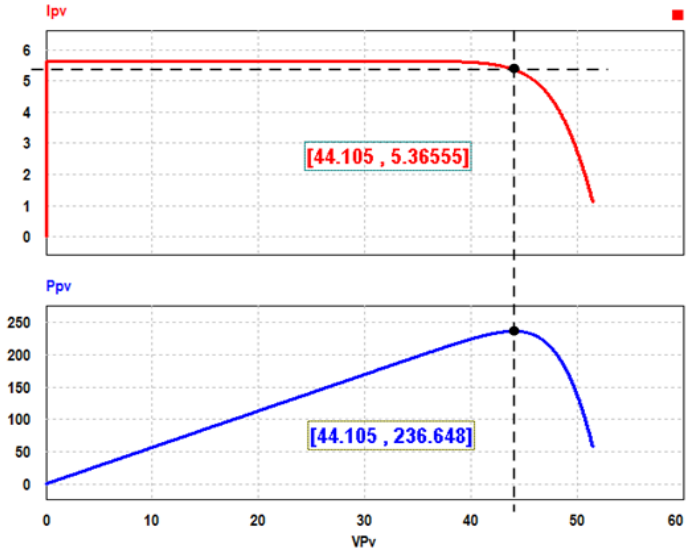

Fig. 14: PV (I-V) characteristics, (P-V) characteristics

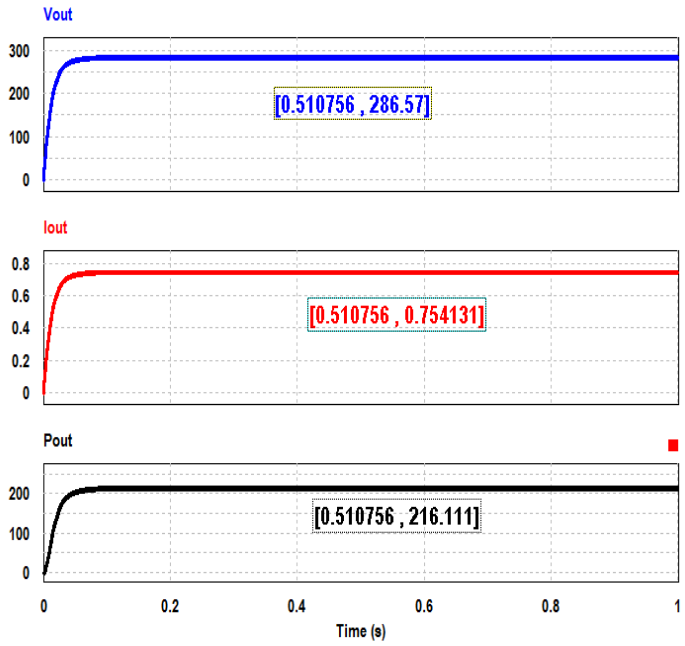

Fig. 15: Waveforms of the output voltage Vout ,the output current Iout ,and the output power Pout

6. CONCLUSIONS

This paper presents a soft switching three-level boost dc-dc converter using an auxiliary resonant. The proposed converter is simulated with various modes of operation and the working principle and the response. This converter is highly efficient because the proposed technique can reduce the switching losses and electromagnetic interference by putting some stress on the devices. Moreover, when either current or voltage is zero during the turning ON or turning OFF periods, then the product of the voltage and current becomes zero, which leads to zero power loss. Therefore, this topology enables the converter to use the low rating switch to improve efficiency. This high-efficiency converter topology provides for the various applications related to renewable energy, and it also can be extended easily to other power conversion systems for satisfying high-voltage demands.

REFERENCES

1- K. Sayed and S. Kown, "A novel quasi-resonant snubber-assisted ZCS-PWM DC-DC converter with high frequency link", Journal of Power Electronics, Vol. 7, No. 2, pp. 1-8, March 2007

2- K. Sayed, M Abdel-Salam, A Ahmed, M Ahmed, "New high voltage gain dual-boost DC-DC converter for photovoltaic power systems", Electric Power Components and Systems 40 (7), 711-728

3- K. Sayed, M Nakaoka, "Performance of Induction Heating Power Supply Using Dual Control Mode Pulse-width Modulation–Pulse-density Modulation High-frequency Inverter", Electric Power Components and Systems 43 (2), 157-166.

4- Irfan Jamil, Zhao Jinquan and Rehan Jamil, "Analysis, Design And Implementation Of Zero-Current-Switching Resonant Converter Dc-Dc Buck Converter" IJEEE, Vol. 2, No. 2, May 2013, 1-12.

5- Milan M. Jovanovic, Michael T.Zhang, Yimin Jiang, Fred C.Lee, "single-phase three level boost power factor correction converter", Proceedings of Tenth Annual Applied Power Electronics Conference and Exposition, APEC '95. Conference, 434 - 439 vol.1, 1995.

6- Kwang-Hwa Liu "zero-voltage switching techniques in dc/dc converter circuits" IEEE, Transactions On Power Electronics, Vol. 5, No. 3. July 1990.

7- A.Suresh Kumar,P.Krishna Reddy "Design & Implementation of Zero Voltage Switching Buck Converter" IJERA, ISSN : 2248-9622, Vol. 4, Issue 9 (Version 5), September 2014, pp.193-198.

8- B. Chitti Babu" Study Of Soft Switching Boost Converter Using An Auxiliary Resonant Circuit" National Institute of Technology Rourkela-769008 (ODISHA) May-2012.

9- Mohammadjavad Baei "A new ZVS-PWM Full-Bridge Boost Converter" ieee,The University of Western Ontario London, Ontario, Canada,2012.

10- A.Mousavi, and G.Moschopoulos,"Soft-Switching DC-DC Converters" in IEEE Trans. on Power Electronics, August 2013.

11- Dib Djalel, Mordjaoui Mourad, and Abdulhabeb Abdulhabeb "A Contribution to Study of a GPV System

MPPT with (P&O) and (FLC) algorithms" (ICSIS'2014) Oct 17-18, 2014 Dubai (UAE).

12- TrishanEsram, Patrick L. Chapman, "Comparison of Photovoltaic Array Maximum Power Point Tracking Techniques", IEEE Transactions on Energy Conversion, vol.22, no.2, pp.439-449, June 2007.

13- G. N. Tiwari and Swapnil Dubey, "Fundamentals of Photovoltaic Modules and Their Applications", Cambridge: Published by The Royal Society of Chemistry, RSC Energy Series no.2, ISBN 978-184-973-020-4, pp.81-107, 2010.

14- C. Liu, B. Wu and R. Cheung "Advanced Algorithm For MPPT Control Of Photovoltaic Systems" Department of Electrical & Computer Engineering, Ryerson University, Toronto, Ontario, Canada M5B 2K3,Montreal, August 20-24, 2004.

15- S.Gomathy, S.Saravanan, Dr. S. Thangavel " Design and Implementation of Maximum Power Point Tracking (MPPT) Algorithm for a Standalone PV System " International Journal of Scientific & Engineering Research Volume 3, Issue 3, March -2012 ISSN 2229-5518

16- Shusmita Rahman, Nadia Sultana Oni, Quazi Abdullah IbnMasud " *Design of a Charge Controller Circuit with Maximum Power Point* Tracker (MPPT) for Photovoltaic System" A Thesis submitted to the Dept. of Electrical & Electronic Engineering, BRAC University in partial fulfillment of the requirements for the Bachelor of Science degree in Electrical & Electronic Engineering, December 15, 2012.

17- K Sayed, M Abdel-Salam, M Ahmed, AA Ahmed, "Modeling and simulation of PV arrays", ASME 2010 International Mechanical Engineering Congress and Exposition, pp. 1-8, 2010.

18- Ja'far Saif Edden Abdel Hafeath Jallad and Marwan Mahmou" Design and Simulation of a Photovoltaic System with Maximum Power Control to Supply a Load with Alternating Current " An-Najah National University Faculty of Graduate Studies, Nablus, Palestine 2012.